International Journal of Mathematics and Computer Applications Research (IJMCAR)
ISSN 2249-6955
Vol.2, Issue 1 Mar 2012 49-90

ONSET OF CONVECTION IN A ROTATING FLUID WITH VARIABLE VISCOSITY

Y. RAMESHWAR[1], A.HARI SINGH NAIK[2] AND ISHAK HASHIM[3]

[1] Department of Mathematics, P.G. College of Science, Saifabad, Hyderabad, 5000 04, India.

[2]Department of Mathematics, University College of Engineering, Osmania University, Hyderabad. 500007, India.

[3] School of Mathematical Sciences, Faculty of Science and Technology, Universiti Kebangsaan, Malaysia, 43600 UKM Bangi Selangor, Malaysia.

ABSTRACT

The problem of rotating natural convective flow about the vertical axis with variable viscosity confined between two horizontal plates is investigated by linear stability analysis. The transformed governing equations are numerically solved by using the Galerkin method. The computed results are compared for special cases with those results of earlier researchers (Chandrasekhar [1] and Stengel et al., [12]) and are found to be in excellent agreement. We have studied both stationary convection and oscillatory convection. The threshold values of Rayleigh number and wave number are computed and presented for various boundary conditions viz. rigid-rigid, rigid-free, free-rigid and free-free and for different values of physical parameters viz., Taylor number Ta, viscosity ratio c and Prandtl number Pr. For rigid-rigid boundary conditions we have studied the effect of c, Ta and Pr on the vertical velocity and temperature eigenfunctions at the onset. It is observed that the rotation rate stabilizes the dynamical system. The occurrence of co-dimension two bifurcation point (CTP) is shown for various boundary conditions.

KEYWORDS: Variable viscosity, Coriolis force, Exponential fluid, Galerkin method.

1. INTRODUCTION

The importance of RBC (Rayleigh-Be´nard convection) with rotation has evinced a significant theoretical and experimental interest in the problem of convection in the rotating fluids and extensively investigated by the pioneering researchers [1]-[9]. The linear stability analysis of RBC in a rotating fluid about the vertical axis with rigid-rigid (R/R), rigid-free (R/F), free-rigid (F/R) and free-free (F/F) boundaries has been thoroughly discussed by Chandrashekar [1] by assuming constant diffusivity coefficients, such as viscosity and thermal conductivity. The authors [1]-[9] have assumed that viscosity as a constant. But for most realistic fluids, the viscosity shows a rather pronounced variation with respect to the temperature. Hence it is necessary to take into account the variation of the viscosity with temperature in order to accurately predict the heat transfer rates.

The problem of temperature dependent variable viscosity has applications in geophysical fluid dynamics especially in mantle convection. In the mantle studies the upper mantle is less viscus than the lower mantle. In the mantle convection Coriolis force exist, but it is small. In the upper mantle the temperature variation controls the behavior of the viscosity, while in the lower mantle it is likely that pressure variations are equally important, since temperature increases rapidly with increasing depth through the lithospere.

The stability of a horizontal layer heated from below has been the subject of extensive study. The natural convection in a horizontal fluid layer with isothermal boundaries and no internal heat sources is governed by the non-dimensional parameter, Rayleigh number R. For a constant viscosity and variable viscosity fluids it is well established that the onset of instability occurs at the critical Rayleigh number predicted by linear theory [1]-[12].

Booker [10] has studied RBC with strongly temperature dependent viscosity. He found experimentally that the convective heat transport in a fluid layer decreases significantly as the ratio of the viscosity, say, c, at the top and bottom boundaries increase. Booker and Stengel [11] have shown that this decrease in the heat transport can be entirely by an increase in the critical Raleigh number with variable viscosity.

Stengel et al. [12] have studied the linear stability analysis of RBC with the temperature dependent viscosity and compared their theoretical results with the experimental results. In their study, they reported that, the critical Rayleigh number is nearly constant for lower values of c then increases, reaches a maximum in the vicinity of $c \approx 8$ and decreases for large c.

In the studies related to the variable viscosity effect, glycerol and its equeous solutions have often been used [13], [14]. Yen-Ming Chen and Pearlstein [15] have considered RBC with variable viscosity. They have compared the critical Rayleigh numbers predicted using the actual viscosity temperature relation $\mu(T)$ to those predicted using simple fits (Arrhenius and exponential approximations) of the data in order to determine the errors associated with these commonly used approximate viscosity variations. Sekhar - Jayalatha [16] also have considered the temperature dependent variable viscosity with two types of liquids namely, Maxwell-Jeffrey and Rivilin-Erickson liquids for RBC problem. They have observed that the effect of variable viscosity parameter destabilizes the system. Rajagopal et al.[17] have investigated RBC in which viscosity is a function of both temperature and pressure. They have studied both linear and nonlinear stability of the problem and shown that the principle of exchange of instability holds. Vanishree and Siddheshwar [18] have considered the non Boussinesq approximation for an anisotropic rotating porous medium occupied by the inversely proportional temperature dependent viscosity to study the onset of stationary convection.

The studies which exist on RBC with variable viscosity do not include the effect of Coriolis force. Hence in the present physical model, we have considered the effect of Coriolis force on RBC with temperature dependent variable viscosity. Addition of the Coriolis force on the RBC introduces another control parameter into the problem, namely, the Taylor number, *Ta*, which is a measure of the rotation rate. This model is an example of double diffusive system, hence one can expect to get either stationary convection or oscillatory convection at the onset.

The linear stability analysis of this physical model is analyzed by using the Galerkin method. We have considered the Galerkin expansion for all dependent variables in terms of orthogonal functions satisfying the various boundary conditions viz., R/R, R/F, F/R and F/F. We present the results of stationary and oscillatory instabilities for different values of Ta, c and Pr for the temperature dependent variable viscosity fluids, namely, the exponential fluids. These exponential fluids are used first by Torrence and Turcotte [19]. The numerical results obtained in the present study are in good agreement with the results of Stengel et al.[12] for the onset of stationary convection in the absence of rotation with variable viscosity. Also for constant viscosity, with or without rotation our results coincide with those of Chandrasekhar [1].

The description of the paper is divided into four parts. In Section 2, the mathematical formulation of the problem is presented. In Section 3, the method of generating the approximate solution by using the Galerkin method is given. In Section 4, the numerical discussions of the results obtained for exponential fluids are presented. Finally, in Section 5, the conclusions of our paper are given.

2. BASIC EQUATIONS

An infinite horizontal fluid layer of depth d which is kept rotating at a constant angular velocity $\vec{\Omega} = \Omega \hat{e}_z$ and is also heated from below is considered,

as shown in Fig.1. Here $\hat{e}_z$ is the unit vector along the axis $\vec{V}'(u', v', w')$ of rotation. It is assumed that the temperature of the lower plate exceeds that of the upper plate by $\Delta T' > 0$. The origin of the coordinate system is assumed to be located in the mid plane of the layer.

We assume that all the physical properties of the fluid are constant except the dynamic viscosity μ and the density ρ. The dynamic viscosity is considered as an arbitrary function of temperature T', as $\mu = \mu_o f(z')$, and the density is taken to be constant except in the body force term of the momentum equation, where it is allowed to depend linearly on temperature as $\rho = \rho_o\left[1-\alpha\left(T'-T'_o\right)\right]$. Here μ_o and ρ_o represent the reference values of μ and ρ, respectively, at the mean temperature T'_o. The perturbed dimensional equations for the rotating Rayleigh-Be´nard system with variable viscosity under the Boussinesq approximation are given by:

the equation of continuity

$$\nabla'.\vec{V}' = 0, \qquad (2.1)$$

the equation of motion

$$\frac{\partial \vec{V}'}{\partial t'} + \left(\vec{V}'.\nabla'\right)\vec{V}' = -\frac{\nabla' P'}{\rho_o} - \vec{\Omega}\times\left(\vec{\Omega}\times\vec{r}'\right) + 2\vec{\Omega}\times\vec{V}' +$$
$$\nabla'.\left[\nu(T').(\nabla'\vec{V}' + (\nabla'\vec{V}')^T)\right] + \alpha g\theta'\hat{e}_{z,} \qquad (2.2)$$

and the heat equation

$$\frac{\partial \theta'}{\partial t'} + \left(\vec{V}'.\nabla'\right)\theta' = \beta w' + \kappa\nabla'^2\theta'. \qquad (2.3)$$

The eq. (2.2) is momentum Nevier-Stokes equation, which describes temporal behavior of perturbation of velocity field $\overline{V}'(u',v',w')$. The second and third terms on the right hand side of eq. (2.2) are respectively the centrifugal and Coriolis forces. In the last term on the right hand side of eq. (2.2), α and g represent the thermal expansion coefficient and acceleration due to gravity, respectively. Next equation of heat conduction (2.3) describes behavior of temperature field perturbation θ' in time.

We use a Cartesian system of coordinates $\vec{r}' = (x', y', z')$ whose dimensional horizontal Coordinates x', y' and vertical coordinate z' are scaled on d. The velocity $\vec{V}'$, the temperature θ', the time t' and the pressure P' are non-dimensionalized by using κ / d, βd, d^2/κ and $\rho_o \kappa d^2$ and are denoted as $\vec{V}, \theta, t$ and P, respectively. Here κ is the thermal diffusivity and β is the adverse temperature gradient.

The variable viscosity, $\nu(z)(=\mu/\rho_o)$ is given by $\nu(z) = \nu_o f(z)$, where ν_o is the reference value of the kinematic viscosity evaluated at T_o and $f\left(=\nu/\nu_o\right)$ is the dimensionless viscosity ratio. For the mantle convective fluid, the temperature dependent viscosity $f(z) = \exp(-cT)$ is an adequate expression over restricted temperature internally and it is used in applications where the pressure dependence can be neglected [20]. We have considered the non-dimensional viscosity variations as

$$f = \exp[c(T_o - T)], \qquad (2.4)$$

Where

$$0 \le \gamma \le 1,\ c = \log\left(\frac{\nu_{\max}}{\nu_{\min}}\right) = \log\left(\frac{1+\gamma}{1-\gamma}\right).$$

The function (2.4) is used by Torrence and Turcotte [19] in their numerical study of finite amplitude convection, and it is called an exponential fluid.

The non-dimensional governing equations in two-dimensions viz. (x,z) – plane are given by

$$\nabla.\vec{V} = 0, \qquad (2.5)$$

$$\frac{1}{\Pr}\left[\frac{\partial}{\partial t} + \left(\nabla.\vec{V}\right)\right]\vec{V} = -\nabla\left(\frac{P}{\Pr} - \frac{Ta\,\Pr}{8}|\hat{e}_z \times \vec{r}|^2\right) +$$
$$f\nabla^2\vec{V} + R\theta\hat{e}_z + Ta^{1/2}\left(\vec{V}\times\hat{e}_z\right) + \hat{e}_x\left[\frac{df}{dz}\left(\frac{\partial w}{\partial x} + \frac{\partial u}{\partial z}\right)\right] +$$
$$\hat{e}_y\frac{df}{dz}\frac{\partial v}{\partial z} + \hat{e}_z\left[\frac{df}{dz}\frac{\partial w}{\partial z}\right], \qquad (2.6)$$

$$\left[\frac{\partial}{\partial t} + \left(\nabla.\vec{V}\right)\right]\theta = w + \nabla^2\theta \qquad (2.7)$$

The dimensionless parameters in the above equations for the description of the motion are, Rayleigh number, $R\,(=\alpha g\Delta T d^3/\kappa\nu_o)$, Prandtl number $\Pr\,(=\nu_o/\kappa)$, Taylor number $Ta\,(=4\Omega^2 d^4/\nu^2{}_o)$ and c.

The z-component of curl of curl of momentum equation and the z-component of curl of momentum equation are given by

$$\left(\frac{1}{\Pr}\frac{\partial}{\partial t}-f\nabla^2\right)\nabla^2 w-2\frac{df}{dz}\nabla^2\frac{\partial w}{\partial z}+$$
$$\frac{d^2 f}{dz^2}\left(\frac{\partial^2}{\partial x^2}-\frac{\partial^2}{\partial z^2}\right)w+R\nabla_h^2\theta+Ta^{1/2}\frac{\partial \omega_z}{\partial z}$$
$$=\hat{e}_z.\frac{1}{\Pr}\left[\nabla\times\nabla\times\left(\vec{V}.\nabla\right)\vec{V}\right], \qquad (2.8)$$

$$\left(\frac{1}{\Pr}\frac{\partial}{\partial t}-f\nabla^2-\frac{df}{dz}\frac{\partial}{\partial z}\right)\omega_z-Ta^{1/2}\frac{\partial w}{\partial z}$$
$$=-\frac{1}{\Pr}\left[\left(\vec{V}.\nabla\right)\omega_z-\left(\vec{\omega}.\nabla\right)w\right] \qquad (2.9),$$

where $\nabla^2=\partial^2/\partial x^2+\partial^2/\partial z^2$ and $\nabla_h^2=\partial^2/\partial x^2$. In the above eqs. (2.8) and (2.9), w and Ω_z denote z-components of velocity and vorticity, respectively. To study the linear stability analysis we write the linear parts of eqs. (2.8), (2.9) and (2.7) as

$$\left(\frac{1}{\Pr}\frac{\partial}{\partial t}-f\nabla^2\right)\nabla^2 w-2\frac{df}{dz}\nabla^2\frac{\partial w}{\partial z}+\frac{d^2 f}{dz^2}\left(\frac{\partial^2}{\partial x^2}-\frac{\partial^2}{\partial z^2}\right)w$$
$$+R\nabla_h^2\theta+Ta^{1/2}\frac{\partial \omega_z}{\partial z}=0, \qquad (2.10)$$

$$\left(\frac{1}{\Pr}\frac{\partial}{\partial t}-f\nabla^2-\frac{df}{dz}\frac{\partial}{\partial z}\right)\omega_z-Ta^{1/2}\frac{\partial w}{\partial z}=0, \qquad (2.11)$$

$$\frac{\partial\theta}{\partial t}=w+\nabla^2\theta. \qquad (2.12)$$

2.1 Boundary Conditions

The physical model given in eqs. (2.10)-(2.12) are analyzed by considering four different types of boundary conditions viz., R/R, R/F, F/R, and F/F for upper and lower boundaries located at z =1/2 and z = - 1/2, respectively. In the abbreviations R/R, R/F, F/R and F/F, the numerator and denominator denote the upper and lower boundaries, respectively. These four types of boundary conditions are given by [1]:

(i) No slip condition on top and bottom boundaries (R/R) i.e.,

$$w = \frac{\partial w}{\partial z} = \theta = \omega_z = 0 \ \ at \ \ z = 1/2, \ z = -1/2 \ . \quad (2.13)$$

(ii) Stress free at top boundary z = 1/2 and no slip at bottom boundary z = - 1/2 (F/R) i.e.,

$$w = \frac{\partial^2 w}{\partial z^2} = \theta = \frac{\partial \omega_z}{\partial z} = 0 \ \ at \ \ z = 1/2, \ w = \frac{\partial w}{\partial z} = \theta = \omega_z$$
$$at \ z = -1/2. \quad (2.14)$$

(iii) No slip at top boundary z = 1/2 and stress free at bottom boundary z = - 1/2 (R/F) i.e.,

$$w = \frac{\partial w}{\partial z} = \theta = \omega_z \ at \ z = 1/2, w = \frac{\partial^2 w}{\partial z^2} = \theta = \frac{\partial \omega_z}{\partial z} = 0$$
$$at \ \ z = -1/2 \ . \quad (2.15)$$

(iv) Stress free condition at top and bottom boundaries (F/F) i.e.,

$$w = \frac{\partial^2 w}{\partial z^2} = \theta = \frac{\partial \omega_z}{\partial z} = 0 \ \ at \ \ z = -1/2, \ z = 1/2 \ . \quad (2.16)$$

2.2 Linear Stability Analysis

In the linear stability theory, the perturbations are assumed to be arbitrarily small and hence the product of perturbations and their derivatives are neglected as compared to the linear terms in the governing equations. Thus we get a system of homogeneous linear differential equations with homogeneous boundary conditions. Therefore, in the linear stability theory, the perturbations can either grow exponentially or the magnitude of the perturbations remains constant. If the perturbations grow exponentially then the system is said to be unstable and if the magnitude remains constant then the system is said to be in the marginal state. By using the normal mode method we have analyzed the stability of this convective system.

Linear eqs. (2.10)-(2.12) can be transformed into ordinary differential equations by writing

$$w(x,z,t) = W(z)\exp(iqx + pt),$$
$$\omega_z(x,z,t) = Z(z)\exp(iqx + pt)$$
$$and$$
$$\theta(x,z,t) = \Theta(z)\exp(iqx + pt), \qquad (2.17)$$

where W(z), Z(z) and $\Theta(z)$ are the eigenfunctions and p denotes the growth rate of the perturbations and q denotes the wave number. Using the above set of solutions (2.17) into eqs. (2.10)-(2.12), we get

$$\frac{p}{\mathrm{Pr}}\left(D^2 - q^2\right)W = (D^2 f)\left(D^2 + q^2\right)W$$
$$+2(Df)(D^2 - q^2)DW + f\left(D^2 - q^2\right)^2 W$$
$$-Rq^2\Theta - Ta^{1/2}DZ, \qquad (2.18)$$

$$\frac{p}{\mathrm{Pr}}Z = f\left(D^2 - q^2\right)Z + DfDZ + Ta^{1/2}DW, \quad (2.19)$$

$$p\Theta = \left(D^2 - q^2\right)\Theta + W, \qquad (2.20)$$

where D denotes differentiation with respect to the vertical coordinate z. The unknown variables W(z), Z(z) and $\Theta(z)$ are expanded in terms of the following complete orthogonal sets of trial functions that satisfy the homogeneous boundary conditions (2.13)-(2.16)

$$W(z) = \sum_{n=1}^{\infty} a_n W_n(z),\ Z(z) = \sum_{n=1}^{\infty} b_n Z_n(z)$$
$$and\ \Theta(z) = \sum_{n=1}^{\infty} c_n \Theta_n(z), \qquad (2.21)$$

Where $W_n(z)$, $Z_n(z)$ and $\Theta_n(z)$ are the trial functions that satisfy the homogeneous boundary conditions (2.13)-(2.16) and the coefficients a_n, b_n and c_n are unknown constants. The trial functions that satisfy the no slip boundary conditions (2.13) are chosen as

$$W_n(z) = \begin{cases} \dfrac{\cosh(\alpha_n z)}{\cosh(\alpha_n/2)} - \dfrac{\cos(\alpha_n z)}{\cos(\alpha_n/2)}, & n\ \ odd, \\ \dfrac{\sinh(\alpha_n z)}{\sinh(\alpha_n/2)} - \dfrac{\sin(\alpha_n z)}{\sin(\alpha_n/2)}, & n\ \ even, \end{cases} \qquad (2.22)$$

where the constants α_n are zeros of

$$\tanh\left(\alpha_n/2\right) + \tan\left(\alpha_n/2\right) = 0, \quad n\ \ odd,$$
$$\coth\left(\alpha_n/2\right) - \cot\left(\alpha_n/2\right) = 0, \quad n\ \ even.$$

The function Z_n is given by

$$Z_n(z) = \begin{cases} \cos(n\pi z), & n \quad odd\,, \\ \sin(n\pi z), & n \quad even, \end{cases} \qquad (2.23)$$

The function Θ_n is given by

$$\Theta_n(z) = \begin{cases} \cos(n\pi z), & n \quad odd\,, \\ \sin(n\pi z), & n \quad even. \end{cases} \qquad (2.24)$$

Similarly, we can choose the trial functions for the remaining boundary conditions viz., R/F, F/R and F/F.

According to the Galerkin method, the residuals are required to be orthogonal to the trial functions. This method is used to obtain an infinite set of linear homogeneous algebraic equations for the unknown coefficients a_n, b_n and c_n in eq. (2.21). In order to obtain a finite number of linear homogeneous algebraic equations, we have truncated the $W(z), Z(z)$ and $\Theta(z)$ expansions in eq. (2.21), say, at M, N and K terms, respectively. After introducing the representations given in eq. (2.21) into eqs. (2.18)- (2.20) and multiplying the resultant equations of (2.18), (2.19) and (2.20) by $W_j, 1 \le j \le M\,; Z_j, 1 \le j \le N$ and $\Theta_j, 1 \le j \le K$, respectively and averaging the result over the fluid layer from $z = -1/2$ to $z = 1/2$ and finally we left with the matrix eigenvalue problem

$$\left(U - pV\right) X = 0, \qquad (2.25)$$

where U, V and X are the matrices and they are given by

$$U=\begin{pmatrix} B_{ji} & C_{ji} & D_{ji} \\ F_{ji} & G_{ji} & H_{ji} \\ J_{ji} & K_{ji} & L_{ji} \end{pmatrix}, V=\begin{pmatrix} A_{ji} & 0 & 0 \\ 0 & E_{ji} & 0 \\ 0 & 0 & I_{ji} \end{pmatrix},$$

$$X=\begin{pmatrix} a_n \\ b_n \\ c_n \end{pmatrix}. \qquad (2.26)$$

The matrix elements in the above eq.(2.26) are defined as

$$A_{ji}=\frac{1}{Pr}\left\langle W_j D^2 W_i - q^2 W_j W_i \right\rangle,$$

$$B_{ji}=\left\langle \ (D^2 f)(W_j D^2 W_i + q^2 W_j W_i)\right.$$

$$+(2Df)(W_j D^3 W_i - q^2 W_j DW_i)+(W_j D^4 W_i$$

$$\left.-2q^2 W_j D^2 W_i + q^4 W_j W_i)\ \right\rangle,$$

$$C_{ji}=-Rq^2\left\langle W_j \Theta_i \right\rangle, \quad D_{ji}=-Ta^{1/2}\left\langle W_j DZ_i \right\rangle,$$

$$E_{ji}=\left\langle \Theta_j \Theta_i \right\rangle,$$

$$F_{ji}=\left\langle \Theta_j W_i \right\rangle, \quad G_{ji}=\left\langle \Theta_j D^2 \Theta_i - q^2 \Theta_j \Theta_i \right\rangle,$$

$$H_{ji}=\left\langle 0 \right\rangle, \quad I_{ji}=\frac{1}{\mathrm{Pr}}\left\langle Z_j Z_i \right\rangle,$$

$$J_{ji}=Ta^{1/2}\left\langle Z_j DW_i \right\rangle, \quad K_{ji}=\left\langle 0 \right\rangle,$$

$$L_{ji}=\left\langle f(Z_j D^2 Z_i - q^2 Z_j Z_i)+(Df)Z_j Z_i \right\rangle,$$

and in general the angular bracket expression represents

$$\left\langle \ldots \right\rangle=\int_{-1/2}^{1/2} h_1(z)h_2(z)dz$$

where $h_1(z)$ and $h_2(z)$ are the orthogonal functions.

The system of eqs. (2.25) is solved as a generalized eigen-value problem and since this is accomplished numerically, this infinite set of equations is made finite by numerical truncation. The real parts of the eigenvalues, say, $\mathrm{Re}(p_k)$ determine the stability of the system. If $\mathrm{Re}(p_k)<0$ for all k, the system is said to be stable. If $\mathrm{Re}(p_k)>0$ for at least one value of k, the system is unstable. The marginal stability curve corresponds to the case when one of the eigenvalues satisfies $\mathrm{Re}(p_k)=0$. The eigenvalue $p=p_k$ is a function of the physical parameters R,q,Ta,c,Pr and $f(z)$. The parameter R determines the onset of instabilities and depends on the physical parameters q,Ta,c,Pr and $f(z)$. At each q the number of eigenvalues depends on the values of M,N and K of trial functions used in eq. (2.21). Only those values of R that are real, positive and finite are considered to be physically meaningful. For the accuracy of R, the trial functions are increased by 2 at a time, until the smallest meaningful R differ by less than 0.1 percentage. We obtain critical value of R by iterating q, until the marginal stable value of R is minimized. The convective system can be unstable to either stationary convection or oscillatory convection at the onset of instability. The occurrence of stationary convection or oscillatory convection in the convective system depends on the physical parameters and also type of the boundary conditions.

(a) Stationary convection

The stationary convection is obtained when $p_k=0$ for some k. The critical Rayleigh number $R=R_{sc}$ and the critical wave number $q=q_{sc}$ for the onset of stationary convection depend on the physical parameters Ta and c. At $R=R_{sc}$ we get pitchfork bifurcation.

(b) Oscillatory convection

The conditions for oscillatory convection are given by $p_k = \pm i\omega$, where, ω is the frequency of the oscillations and $\omega^2 > 0$. The critical Rayleigh number $R = R_{oc}$ and the critical wave number $q = q_{oc}$ for various types of boundary conditions are computed when $\omega^2 > 0$. The threshold values R_{oc} and q_{oc} depend on $Ta, \Pr$ and c. For the present physical system we have observed that the overstability can occur when the $\Pr$ is small. The time dependent convective flow exists when $R = R_{oc}$ and $R = R_{oc}$ corresponds to Hopf bifurcation.

The pitchfork and Hopf bifurcations are known as primary bifurcations. The secondary bifurcations viz., Takens-Bogdanov bifurcation point $(\omega^2 = 0)$ and co-dimension two bifurcation point (CTP) ($\omega^2 > 0$) occur on combining Rayleigh numbers and wave numbers of stationary convection and oscillatory convection. At CTP, we get $R_{sc} = R_{oc}$ but $q_{sc} \neq q_{oc}$. The intersection point of the neutral curves of stationary convection and oscillatory convection in the (c, R_c)-plane gives CTP and it is discussed in detail in the next section.

3. NUMERICAL RESULTS AND DISCUSSION

In this section the attention has been paid for the effect of physical parameters such as Ta, c and $\Pr$ on the threshold values of R_{sc}, q_{sc}, R_{oc} and q_{oc} for various boundary conditions. In particular for R/R boundary conditions the effect of Ta, c and $\Pr$ on eigenfunctions, namely, $W(z)$ and $\Theta(z)$ are plotted and discussed.

The RBC model either with constant viscosity or variable viscosity is unstable to only stationary convection at the onset. The numerically computed

results of stationary convection and oscillatory convection are plotted in Figs. (2)-(10). In these figures each solid line corresponds to stationary convection and each dotted line corresponds to oscillatory convection. The difference in the instability between the fluid with constant viscosity $(c=0)$ and the fluid with temperature dependent variable viscosity $(c\neq 0)$ is shown in the Figs. (2)-(7). In these figures, the neutral curves start from the vertical axis and the values on the vertical axis give the constant viscosity results corresponding to $c=0$. These results for $c=0$ and for all values of Ta coincide with those of Chandrasekhar [1].

We denote the critical Rayleigh number and critical wave number for the stationary convection with variable viscosity ($c\neq 0$) as $R=R_{sc}^{v}$ and $q=q_{sc}^{v}$, respectively. Similarly we denote the critical Rayleigh number and the critical wave number for the oscillatory convection with variable viscosity as $R=R_{oc}^{v}$ and $q=q_{oc}^{v}$, respectively. R_{sc}^{c} and q_{sc}^{c} stand for critical Rayleigh number and critical wave number, respectively, for the onset of stationary convection when $c=0$. Finally R_{oc}^{c} and q_{oc}^{c} stand for critical Rayleigh number and critical wave number, respectively, for the onset of oscillatory convection when $c=0$.

The onset of stationary convection is plotted in the Figs. 2 and 3 in (c,R_{sc})-plane (c,q_{sc})-plane, respectively, for various boundary conditions, viz., R/R, R/F, F/R, F/F. In these figures, the effect of $Ta=(0\,and\,1000)$ and $0\leq c\leq 16$ are studied for large Pr. From these Figs. 2(a-d) it is observed for R/R, R/F, F/R, F/F boundary conditions, R_{sc}^{c} and R_{sc}^{v} increases as Ta increase. This result shows that the Coriolis force stabilizes the onset of stationary convection. From Fig. 3, we can observe that as Ta increases q_{sc}^{c} and q_{sc}^{v}

increase for all boundary conditions. This result shows that the wave length of the roll pattern decreases as the rotation rate increases.

Also in Figs. 2 and 3, the effect of c on the threshold values is shown. For a given Ta, Fig. 2 shows that as c increases the values of R_{sc} increase and approaches to a peak point. The value of c at the peak point is denoted as $c = c^*$. When the parameter c increases and $c < c^*$, then R_{sc}^v increases and $R_{sc}^v > R_{sc}^c$. For $c > c^*$ and as c increases, the values of R_{sc}^v starts to decrease. Hence, for the values $c < c^*$ and the increment in c inhibits the onset of stationary convection for a given Ta. For the values of $c > c^*$ and the increment in c destabilizes the convective system for a given Ta. The decrease of R_{sc}^v in the region of sufficiently large viscosity variation ($c > c^*$) is related to the fact that a transition takes place in the fluid region from motions involving the whole layer thickness to those located in a certain low viscosity sublayer. In the absence of rotation ($Ta = 0$) for $c > 8$, as c increases the R_{sc}^v for the boundaries R/R and F/R coincide and also the same holds for the boundaries R/F and F/F. For all the boundary conditions the q_{sc}^v coincide for large values of c. The above results for $Ta = 0$ coincide with that of Stengel et al. [12]. Whereas in the presence of Coriolos force ($Ta \neq 0$) the situation is not the same which we can observe in Figs. 2 and 3. We have observed that for small values of Ta, the system is unstable to only stationary convection for the given values of remaining physical parameters. For large values of Ta and $\mathrm{Pr} < 1$, the system can be unstable to oscillatory convection and these results are shown in Figs. (4)-(7).

We have studied the effect of Pr on the onset of oscillatory convection for all boundary conditions in Figs. 6 and 7 for $Ta = 10^4$. Figure 6, shows that as Pr

increases, the onset of oscillatory convection increase for all boundary conditions. From these Figs. 6(a-d), we conclude that increasing values of $\Pr$ stabilizes the convective system. Figure 6(a) is plotted for R/R boundaries and it shows that for $\Pr = 0.025$ and for all values of c, we get oscillatory convection as a first instability. But for $\Pr = 0.1$ and for small values of c we get stationary convection as a first instability and for higher values of c we get oscillatory convection as a first instability. Figures 6(b) and 6(c) are plotted for R/F and F/R boundaries, respectively, and they show that, for small values of c, we get stationary convection as a first instability, further as c increases, we get oscillatory convection as a first instability. Figure 6(d) is drawn for F/F boundaries and shows that for all values of c, we always get oscillatory convection as a first instability for the given values of Pr. The occurrence of stationary convection or oscillatory convection as a first instability also depends on the type of the boundary conditions for large Ta and $\Pr < 1$. Figure 7 show that as $\Pr$ increases, the q_{oc}^{c} and q_{oc}^{v} also increase for all boundary conditions. From Fig.7 it also observed that the critical wave numbers of stationary convection are higher than that of oscillatory convection except for the R/F boundary conditions (Fig.7b). From the set of figures (Fig. 6(a), Fig. 7(a)) and (Fig. 6(c), Fig. 7(c)) the CTP is observed for $\Pr = 0.1$. From the set of figures (Fig. 6(b), Fig. 7(b)) and (Fig. 6(c), Fig. 7(c)) the CTP is observed for $\Pr = 0.025$. This occurrence of CTP can also be observed in Figs. 4 and 5.

The temperature dependence of viscosity can also effect the vertical flow structure. To cause considerable changes in the vertical distribution of convection velocity, this dependence must be sufficiently large. We have numerically calculated the vertical velocity eigenfunction $W(z)$ and temperature eigenfunction $\Theta(z)$ at the critical bifurcation point for different values of Ta, $c, \Pr$ and for R/R boundary conditions. Figure 8 is plotted for the

eigenfunctions $W(z)$ and $\Theta(z)$ at the onset of stationary convection. Figures 8(a,c) are plotted for $Ta = 10^4$ and different values of c. Figures 8(b,d) are plotted for $c = 7$ and $Ta = 0, 10^4$. In Figs. 8(a) and 8(b), we have studied the effect of c and Ta on $W(z)$, respectively. Fig. 8(a) shows that, as c increases $W(z)$ attains the maximum value in the low viscosity region. As c increases the region of the lower viscosity is nearer to the bottom and this maximum appears in the region of low viscosity. The effect of Coriolis force (Ta) shows that the maximum value of $W(z)$ moves away from the lower boundary [see Fig. 8(b)].

The effect of c and Ta on the $\Theta(z)$ are shown in Figs. 8(c) and 8(d), respectively. The eigenfunction $\Theta(z)$ is the first order temperature perturbation. Like all the temperature perturbation functions, $\Theta(z)$ must vanish on the boundary of the fluid layer since the boundaries are isothermal. From Fig. 8(c) it is observed that for $c = 0, \Theta(z)$ is symmetric about the midpoint of the layer. Also it is observed that as c increases, the temperature perturbation becomes confined to a small region near the bottom of the layer where the fluid is less viscous. The effect of Coriolis force (Ta) shows that the maximum value of $\Theta(z)$ moves away from the lower boundary [see Fig. 8(d)].

Figure 9 is plotted for $W(z)$ and $\Theta(z)$ at the onset of oscillatory convection for R/R boundary conditions. Figures 9(a,c) are plotted for $Ta = 10^4$ and for different values of c. Figures 9(b,d) are plotted for $c = 7$ and $Ta = 10^4$ and $Ta = 10^5$. In Figs. 9(a) and 9(b), we have studied the effect of c and Ta on $W(z)$, respectively. It is observed that the behavior of $W(z)$ at the onset of oscillatory convection is similar to that of stationary convection. The effect of c and Ta on $\Theta(z)$ are shown in Figs. 9(c) and 9(d), respectively. From Fig. 9(c) it

is observed that as c increases, the $\Theta(z)$ becomes confined to a small region near to the bottom of the layer where the fluid is less viscous. Figure 9(d) shows as the Coriolis force (Ta) decreases $\Theta(z)$ takes maximum value in the low viscosity region for a constant c.

Figures 10(a) and 10(b) show the effect of Pr on $W(z)$ and $\Theta(z)$, respectively, at the onset of oscillatory convection for $Ta = 10^4$, $c = 7$ and R/R boundary conditions. From Fig. 10(a) we can observe that as Pr decreases $W(z)$ where it takes the maximum value is in the low viscosity region and the same is true in the case of $\Theta(z)$ [see Fig. 10(b)].

4. CONCLUSIONS

The onset of stationary convection and oscillatory convection of rotating variable viscosity fluid in a horizontal layer has been studied for different types of boundary conditions by using the Galerkin method. We have considered the variable viscosity fluid as exponential fluid. For rigid-rigid (R/R) boundary conditions, we have computed vertical velocity eigenfunction $W(z)$ and temperature eigenfunction $\Theta(z)$ at the onset. For this physical model we have observed that the convective system can be unstable to either stationary convection or oscillatory convection and depends on the physical parameters Ta, Pr and c. For $Ta = 0$ and small values of Ta the present buoyancy driven convective system exhibits only stationary convection at the onset for the boundary conditions R/R, R/F, F/R, F/F and for all values of c.

The computed threshold values of stationary convection for all combinations of boundary conditions when $Ta = 0, c = 0$ and $Ta = 0, c \neq 0$ are in good agreement with those of Chandrashekar[1] and Stengel et al.[12], respectively. For $Ta \neq 0, c = 0$ the threshold values of convection are also in

good agreement with those of Chandrashekar [1]. We have obtained the oscillatory convection for small values of $\mathrm{Pr}(\mathrm{Pr}<1)$ and large values of Ta. It is observed that as Ta increases the onset of convection increase. This implies that the rotation rate inhibits the onset of convection. Also as Ta increases the critical wave numbers of stationary convection and oscillatory convection increase. This result shows that the wave length of the roll pattern decrease as Ta increases. From (c, R_{sc}) - plane it is observed that for $c<c^*$ (value of c at the peak point), the onset of convection increases. This implies that the viscosity variation when $c<c^*$ shows the stabilizing effect. Similarly the system shows the destabilizing effect for the increment values of c and $c>c^*$. The peak point (c^*) of viscosity ratio is also depends on the rotation rate. The Prandtl number is an important parameter to get overstability. The effect of Pr shows that as Pr increases the onset of oscillatory convection increases. The occurrence of co-dimension two bifurcation point is observed for the considered values of the physical parameters.

The effect of c and Ta on $W(z)$ and $\Theta(z)$ at the onset of stationary convection for R/R boundary conditions are studied. It is noticed that as c increases $W(z)$ takes maximum value in the low viscosity region and the opposite effect is observed as Ta increases. The maximum value of $\Theta(z)$ occurs near the lower boundary as a parameter c but as Ta increases the maximum value of $W(z)$ moves upwards from the lower boundary. We have also studied the effect of c, Ta and Pr on $W(z)$ and $\Theta(z)$ at the onset of oscillatory convection. The eigenfunctions $W(z)$ and $\Theta(z)$ of oscillatory convection behave in a similar manner as those of stationary convection. Finally,

the effect of Pr is same as the effect of Ta on $W(z)$ and $\Theta(z)$ at the onset of oscillatory convection.

REFERENCES

1. S. Chandrashekar, Hydrodynamic and Hydromagnatic stability, Oxford: Clarendon. (1961)
2. F.H. Busse and R.M. Clever, “Nonlinear properties of convection rolls in a horizontal layer rotating about a vertical axis”, J. Fluid Mech. Vol. 94, (1979), pp.609.
3. G. K\"uppers and D. Lortz, “Transition for laminar convection to thermal turbulence in rotating fluid layer”, J. Fluid Mech. Vol.35, (1969), pp.609.
4. F.H. Busse and K.E. Heikes, “Convection in a rotating layer : A simple case of turbulence”, Science, Vol.208, (1980), pp.173.
5. J.J. Niemela and R.J. Donnelly, “Direct transition to turbulence in rotating Be`nard convection”, Phys. Rev. Lett., Vol. 57, (1986), pp.2524.
6. T. Clune and E. Knobloch, “Pattern sellection in rotating convection with experimental boundary conditions”, Phys. Rev. E., Vol. 47, (1993), pp.2536.
7. E. Knobloch, “Rotating convection : Recent developments”, Int. J. Engg. Sci., Vol. 36, (1998), pp.1421.
8. E. Knobloch and M. Silber, “Travelling wave convection in a rotating layer”, Geophys. Astrophys. Fluid Dyn., Vol. 51, (1990), pp.195.
9. S.G. Tagare, A. Benerji Babu and Y. Rameshwar, “Rayleigh-Be`nard convection in rotating fluids”, Int. J. Heat Mass Trans., Vol. 51, (2008), pp.1168.

10. J.R. Booker, “Thermal convection with strongly temperature dependent viscosity”, J. Fluid Mech., Vol. 76, (1976), pp.741.

11. J.R. Booker and K.C. Stengel, “Further thoughts on convective heat transport in variable viscosity fluids”, J. Fluid Mech., Vol. 86, (1978), pp.289.

12. K.C. Stengel, D.S. Oliver and J.R. Booker, “Onset of convection in a variable viscosity fluid”, J. Fluid Mech., Vol. 120, (1982), pp.411.

13. D.R.Jakins, “Rolls versus squares in thermal convection of fluids with temperature dependent viscosity”, J. Fluid Mech., Vol. 178, (1987), pp. 491.

14. S.Thanham and C.F. Chen, “Stability analysis on the convection of a variavle viscosity fluid in an infinite vertical slot”, Phys. Fluids, Vol. 29, (1986), pp.1367.

15. Yen-Ming Chen and Arne J. Pearlstein, “Onset of convection in a variable viscosity fluids: Assesment of approximate viscosity-temperature relations”, Phys. of Fluids, Vol.31, (1988), pp.1380.

16. G.N. Sekhar and G. Jayalatha, “Elastic Effects on Rayleigh-B\'enard convection in liquids with temperature dependent viscosity”, Int. J. Ther. Sci., Vol. 49, (2010), pp.67.

17. K.R. Rajagopal, G. Saccomandi and L. Vergori, “Stability Analysis of the Rayleigh-Be`nard convection for a fluid with temperature and pressure dependent viscosity”, ZAMP, Vol. 60, (2009), pp.739.

18. R.K.Vanishree and P.G.Siddheshwar, “Effect of rotation on thermal convection in an anisotropic porous medium with temperature dependent viscosity”, Transp Porous Med., Vol. 81, (2010), pp.73.

19. K.E. Torrence and D.L. Turcotte, “Thermal convection with large viscosity variation”, J. Fluid Mech., Vol. 47, (1971), pp.113.

20. G. Schubert, D.L. Turcotte and P. Oslon, “Mantle convection in the Earth and Planets, Taylor and Francies”, Newyork (2004) (Chapters 5, 9, 13).

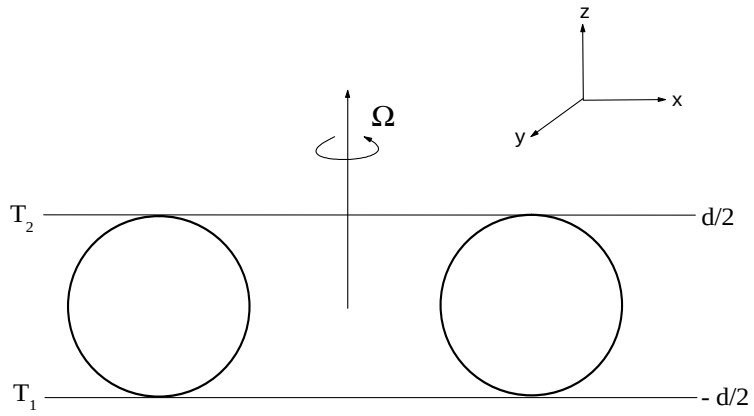

Figure 1 : The schematic diagram of the physical configuration.

T_1 and T_2 represent the temperatures at the lower and upper boundaries respectively.

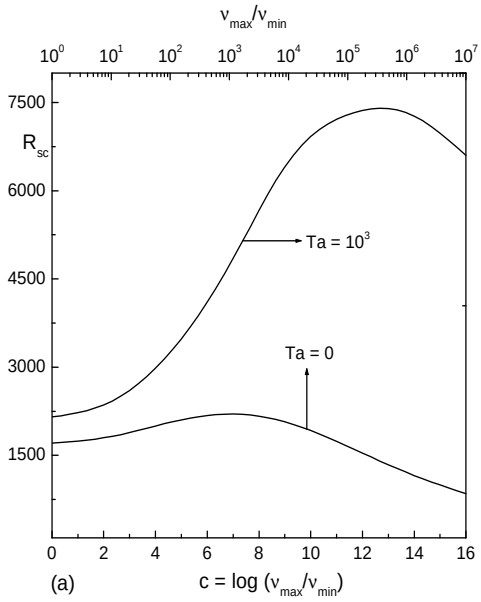
ν_{max}/ν_{min}
10^0 10^1 10^2 10^3 10^4 10^5 10^6 10^7
7500
R_{sc}
6000
4500
3000
1500
Ta = 10^3
Ta = 0
0 2 4 6 8 10 12 14 16
(a)
c = log (ν_{max}/ν_{min})

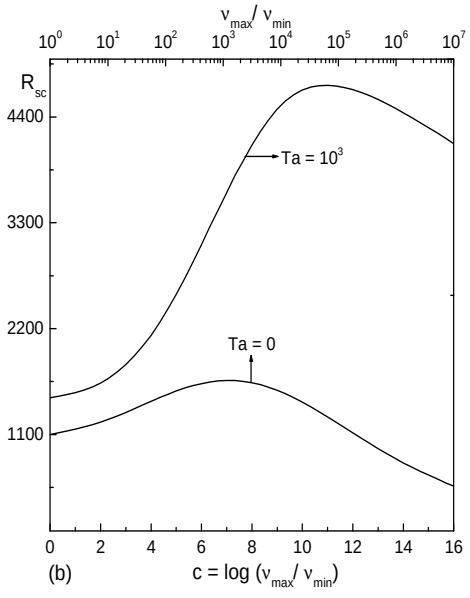
ν_{max}/ν_{min}
10^0 10^1 10^2 10^3 10^4 10^5 10^6 10^7
R_{sc}
4400
3300
2200
1100
Ta = 10^3
Ta = 0
0 2 4 6 8 10 12 14 16
(b)
c = log (ν_{max}/ν_{min})

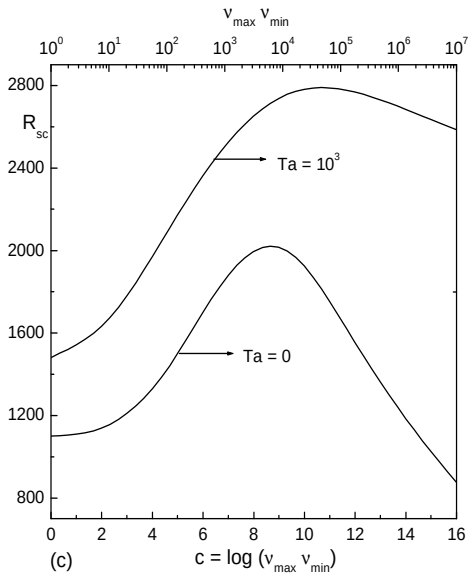

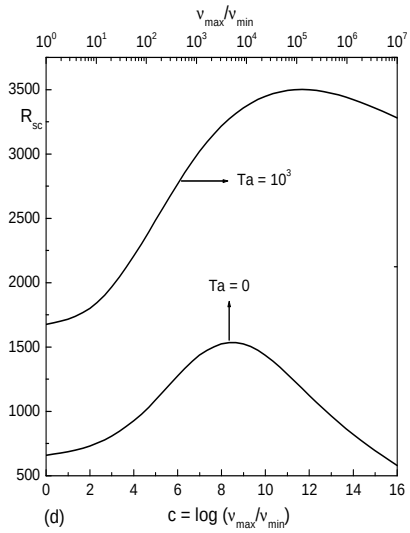

Figure 2 : (c,R_{sc})-plots of neutral stability curves at the onset of stationary convection for different values of *Ta* and large *Pr* with (a) R/R, (b) R/F, (c) F/R, (d) F/F boundary conditions

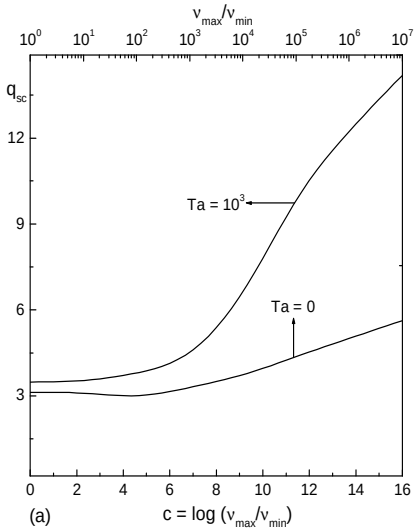
ν_{max}/ν_{min}
10^0 10^1 10^2 10^3 10^4 10^5 10^6 10^7
q_{sc}
12
9
6
3
Ta = 10^3
Ta = 0
0 2 4 6 8 10 12 14 16
(a)
c = log (ν_{max}/ν_{min})

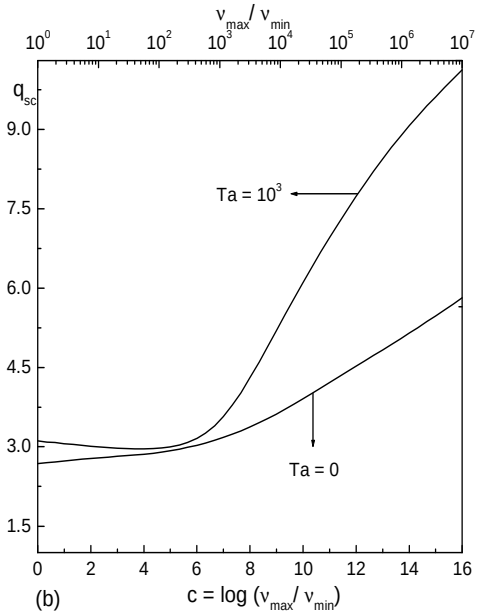
ν_{max}/ν_{min}
10^0 10^1 10^2 10^3 10^4 10^5 10^6 10^7
q_{sc}
9.0
7.5
6.0
4.5
3.0
1.5
Ta = 10^3
Ta = 0
0 2 4 6 8 10 12 14 16
(b)
c = log (ν_{max}/ν_{min})

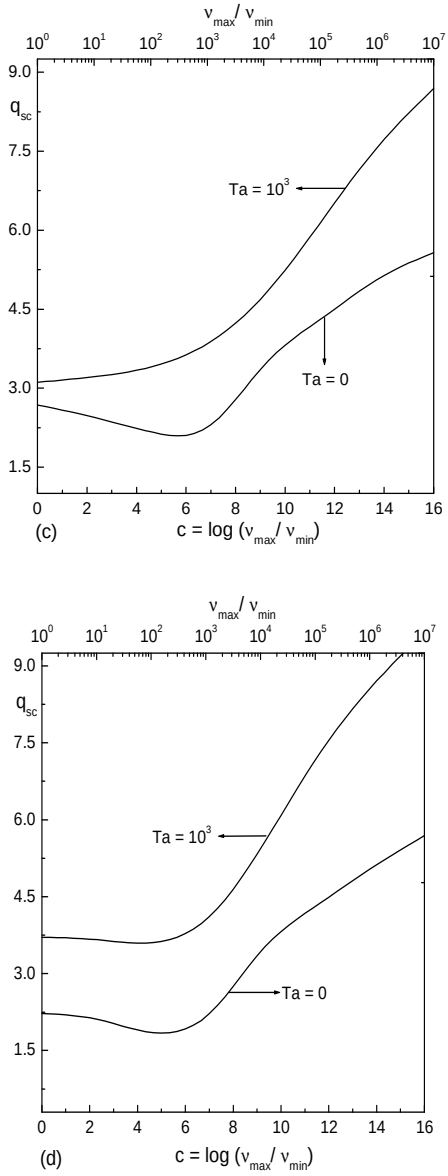

Figure 3 : **(c,q_{sc})-plots of wave number curves at the onset of stationary convection for different values of *Ta* and large *Pr* with (a) R/R, (b) R/F, (c) F/R, (d) F/F boundary conditions**

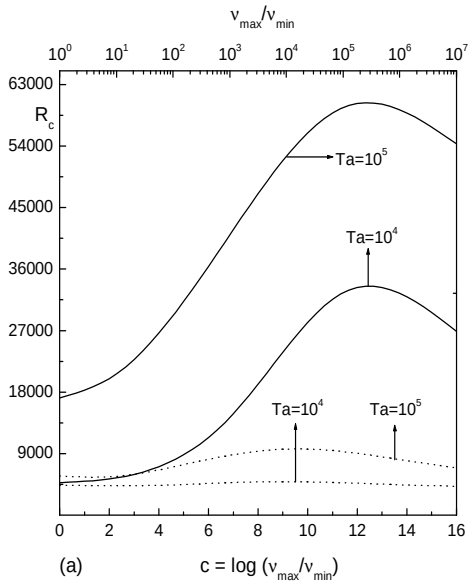
νmax/νmin
10^0 10^1 10^2 10^3 10^4 10^5 10^6 10^7
63000
Rc
54000
45000
36000
27000
18000
9000
Ta=10^5
Ta=10^4
Ta=10^4
Ta=10^5
0 2 4 6 8 10 12 14 16
(a)
c = log (νmax/νmin)

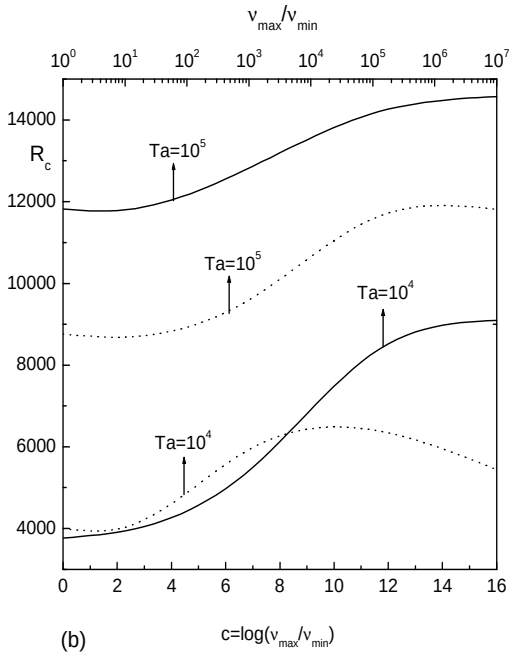
νmax/νmin
10^0 10^1 10^2 10^3 10^4 10^5 10^6 10^7
14000
Rc
12000
10000
8000
6000
4000
Ta=10^5
Ta=10^5
Ta=10^4
Ta=10^4
0 2 4 6 8 10 12 14 16
(b)
c=log(νmax/νmin)

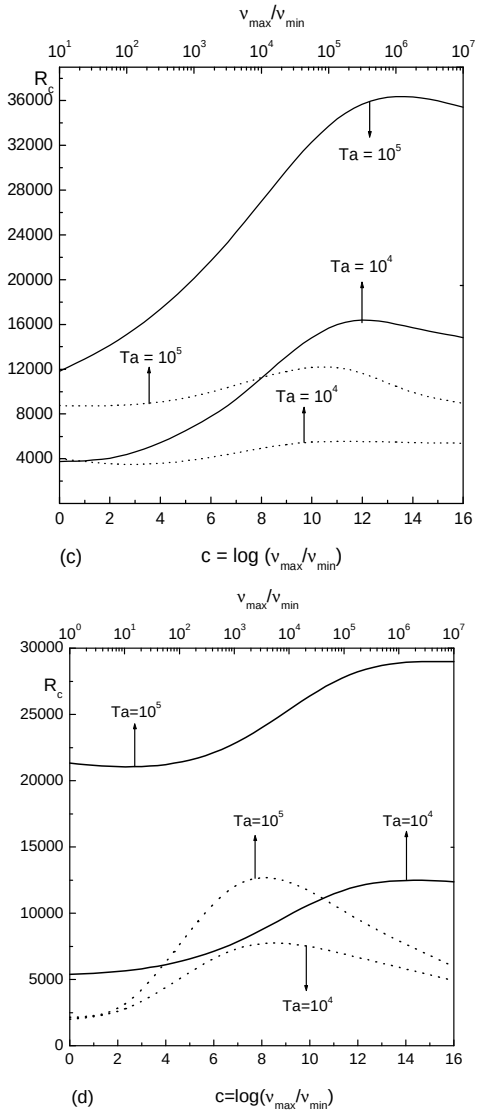

Figure 4 : ***(c,R_c)*-plots of neutral stability curves of stationary convection (solid lines) and oscillatory convection (dotted lines) with (a) R/R, (b) R/F, (c) F/R, (d) F/F boundaries and *Ta=10^4, 10^5*. The dotted lines are plotted for *Pr=0.025***

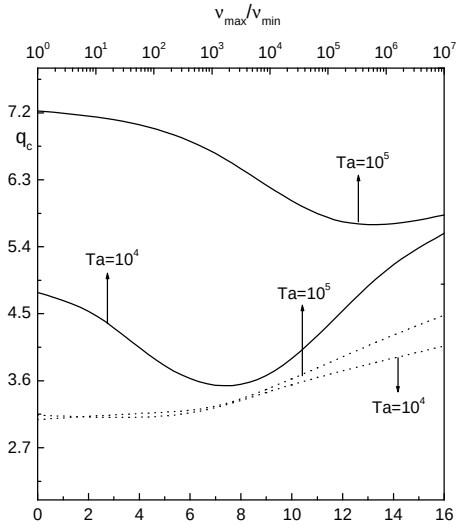
νmax/νmin
10^0 10^1 10^2 10^3 10^4 10^5 10^6 10^7
7.2
qc
6.3
5.4
4.5
3.6
2.7
Ta=10^5
Ta=10^4
Ta=10^5
Ta=10^4
0 2 4 6 8 10 12 14 16
(a)
c = log (νmax/νmin)

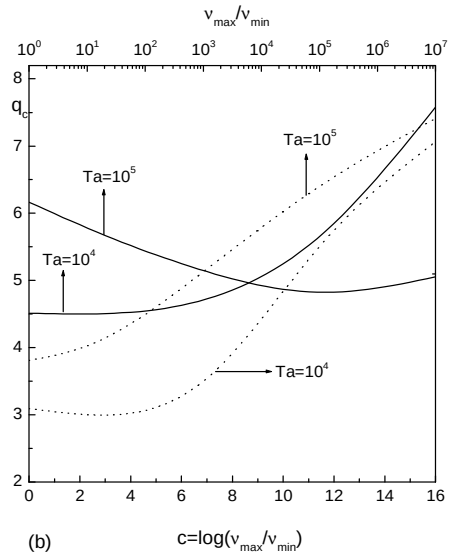
νmax/νmin
10^0 10^1 10^2 10^3 10^4 10^5 10^6 10^7
8
qc
7
6
5
4
3
2
Ta=10^5
Ta=10^5
Ta=10^4
Ta=10^4
0 2 4 6 8 10 12 14 16
(b)
c=log(νmax/νmin)

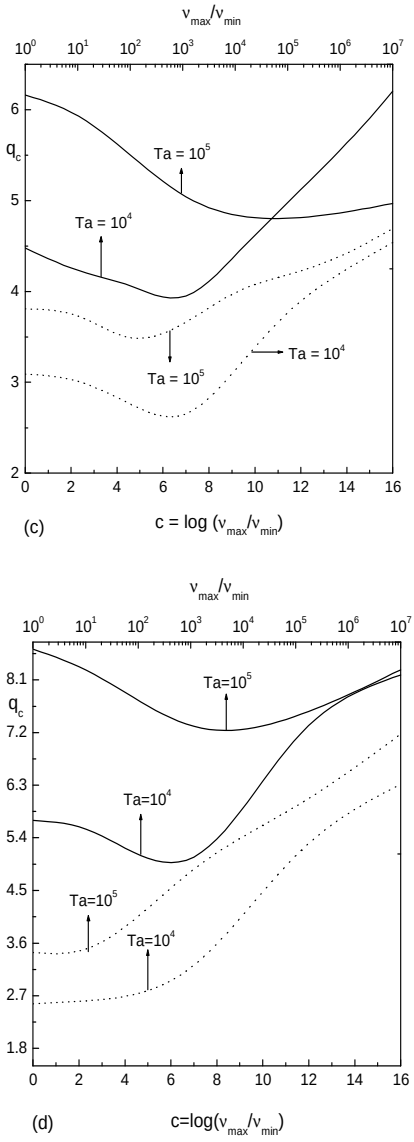

Figure 5 : ***(c,q_c)*-plots of threshold values of wave number for stationary convection (solid lines) and oscillatory convection (dotted lines) with (a) R/R, (b) R/F, (c) F/R, (d) F/F boundaries and *Ta=10^4,10^5*. The dotted lines are plotted for *Pr=0.025*.**

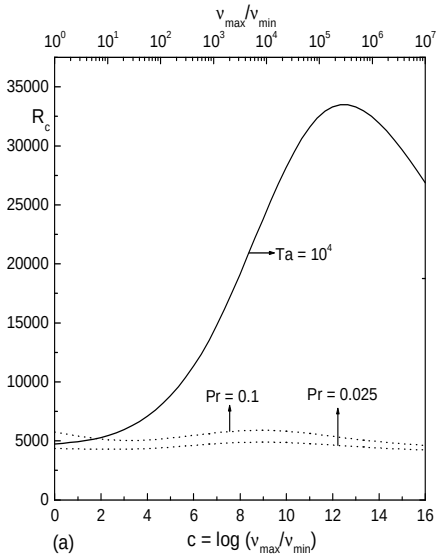
v_{max}/v_{min}
10^0 10^1 10^2 10^3 10^4 10^5 10^6 10^7
35000
R_c
30000
25000
20000
15000
10000
5000
0
Ta = 10^4
Pr = 0.1
Pr = 0.025
0 2 4 6 8 10 12 14 16
(a)
c = log (v_{max}/v_{min})

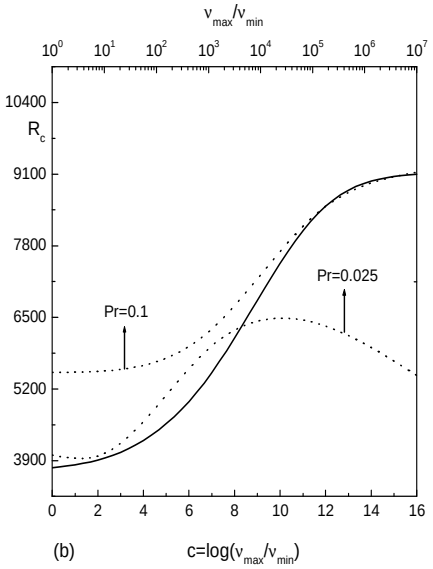
v_{max}/v_{min}
10^0 10^1 10^2 10^3 10^4 10^5 10^6 10^7
10400
R_c
9100
7800
6500
5200
3900
Pr=0.1
Pr=0.025
0 2 4 6 8 10 12 14 16
(b)
c=log(v_{max}/v_{min})

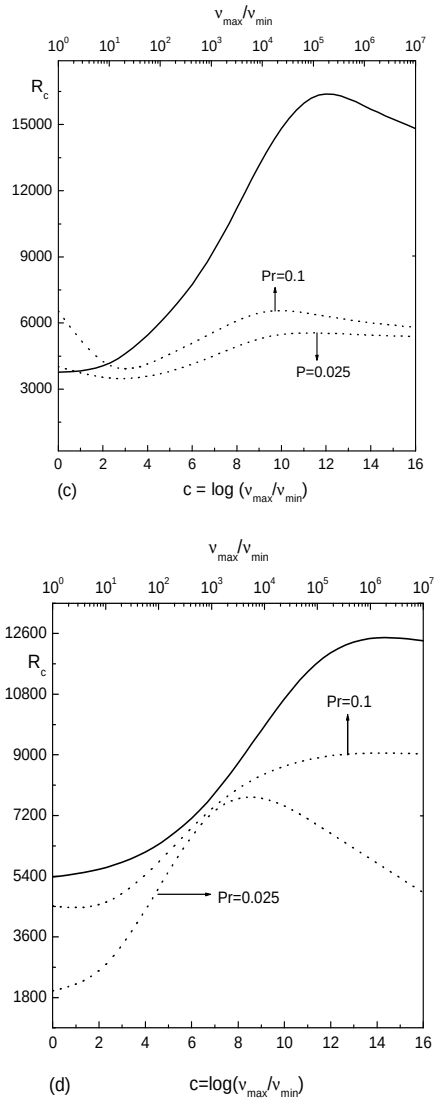

Figure 6 : ***(c,R_c)*-plots of neutral stability curves of stationary convection (solid lines) and oscillatory convection (dotted lines) for (a) R/R, (b) R/F, (c) F/R, (d) F/F boundaries and $Ta=10^4$.**

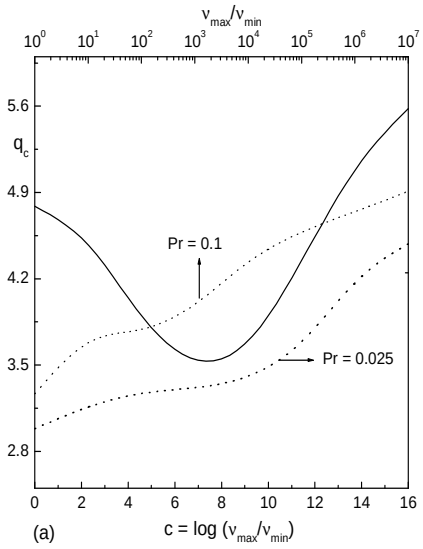
ν_{max}/ν_{min}
10^0 10^1 10^2 10^3 10^4 10^5 10^6 10^7
5.6
q_c
4.9
4.2
3.5
2.8
Pr = 0.1
Pr = 0.025
0 2 4 6 8 10 12 14 16
(a)
c = log (ν_{max}/ν_{min})

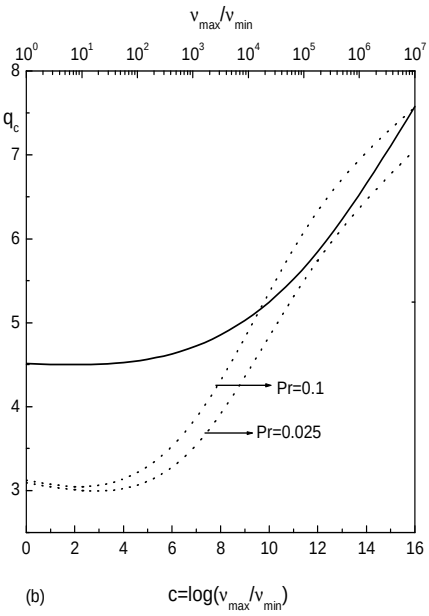
ν_{max}/ν_{min}
10^0 10^1 10^2 10^3 10^4 10^5 10^6 10^7
8
q_c
7
6
5
4
3
Pr=0.1
Pr=0.025
0 2 4 6 8 10 12 14 16
(b)
c=log(ν_{max}/ν_{min})

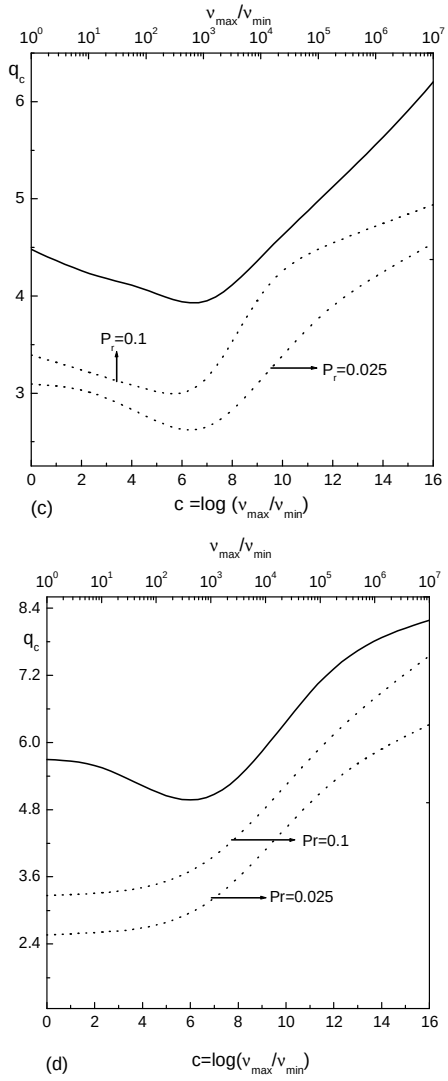

Figure 7 : ***(c,q_c)*-plots of threshold wave numbers of stationary convection (solid lines) and oscillatory convection (dotted lines) with (a) R/R, (b) R/F, (c) F/R, (d) F/F boundaries and $Ta=10^4$.**

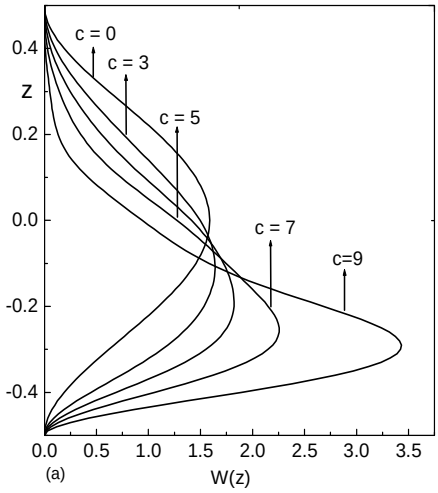
c = 0
c = 3
c = 5
c = 7
c=9
z
0.4
0.2
0.0
-0.2
-0.4
0.0 0.5 1.0 1.5 2.0 2.5 3.0 3.5
W(z)

(a)

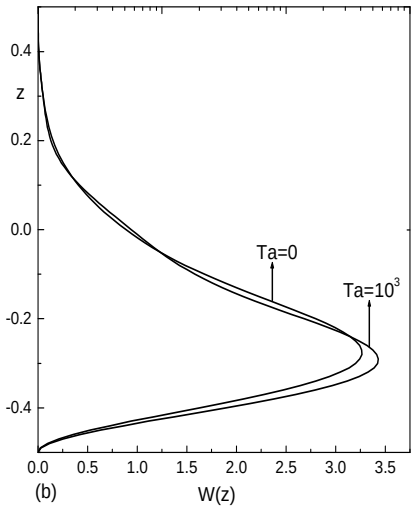
Ta=0
Ta=10^3
z
0.4
0.2
0.0
-0.2
-0.4
0.0 0.5 1.0 1.5 2.0 2.5 3.0 3.5
W(z)

(b)

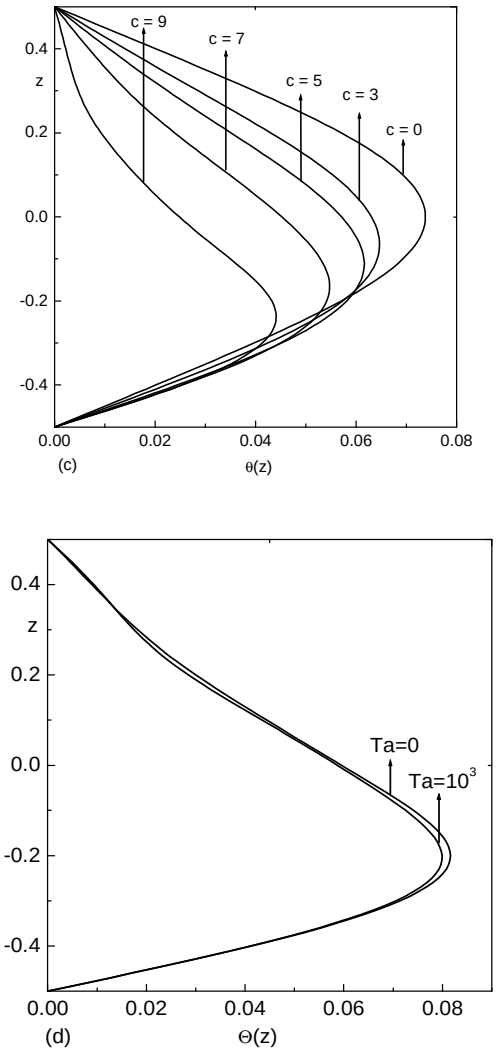

Figure 8 : **Plots of *W(z)* (a), (b) and $\Theta(z)$ (c), (d) vs vertical axis *z* for different values of *c* and *Ta* with R/R boundary conditions at the onset of stationary convection**

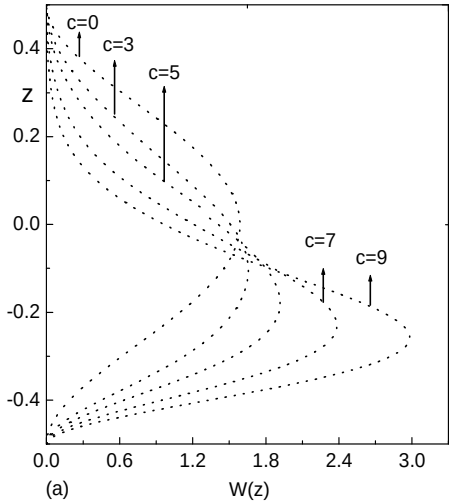
c=0
c=3
c=5
c=7
c=9
Z
0.4
0.2
0.0
-0.2
-0.4
0.0
0.6
1.2
1.8
2.4
3.0
(a)
W(z)

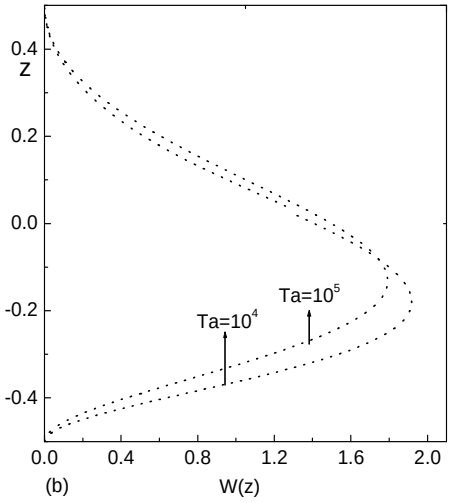
Ta=10^5
Ta=10^4
Z
0.4
0.2
0.0
-0.2
-0.4
0.0
0.4
0.8
1.2
1.6
2.0
(b)
W(z)

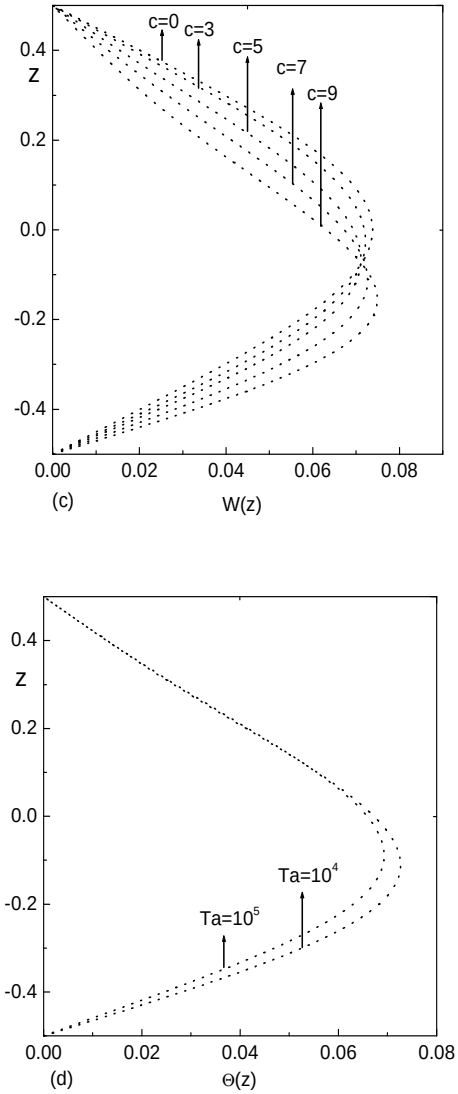

Figure 9 : **Plots of *W(z)* (a), (b) and $\Theta(z)$ (c), (d) vs vertical axis *z* for different values of *c*, *Ta* and *Pr=0.025* with R/R boundary conditions at the onset of oscillatory convection**

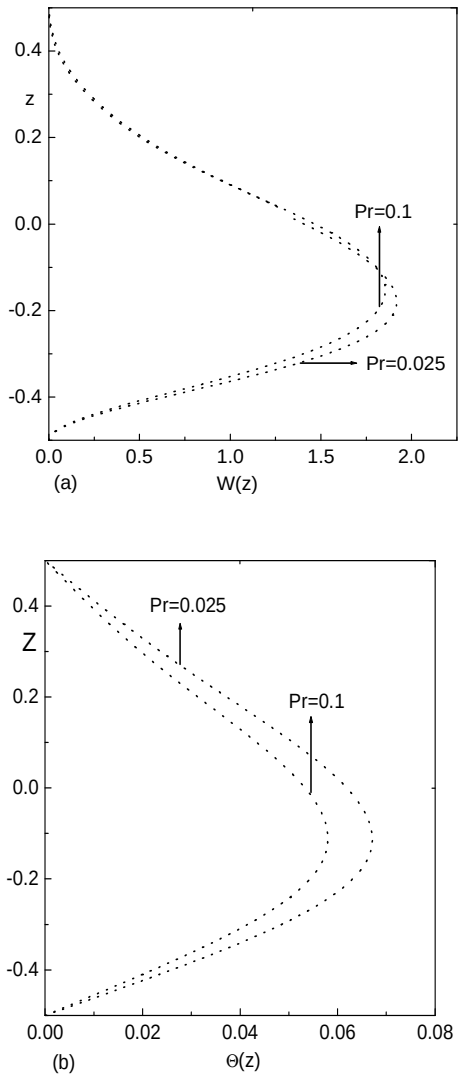

Figure 10 : ***Plots of W(z)*** **(a) and** $\Theta(z)$ **(b) vs vertical axis** ***z*** **for different values of** ***Pr, Ta=10^4*** **and** ***c = 7*** **with R/R boundary conditions at the onset of oscillatory convection**

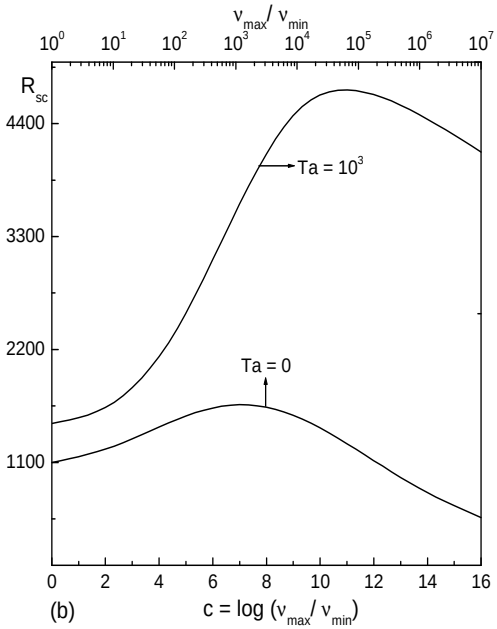
ν_{max}/ν_{min}
10^0 10^1 10^2 10^3 10^4 10^5 10^6 10^7
R_{sc}
4400
3300
2200
1100
Ta = 10^3
Ta = 0
0 2 4 6 8 10 12 14 16
(b)
c = log (ν_{max}/ν_{min})